

Asymmetric Dark Matter and the Scalar–Tensor Model

Shun-Zhi Wang^{a*}, Hoernisa Iminniyaz^{b†}, Mamatrishat Mamat^{c‡},

^a*College of Fundamental Studies, Shanghai University of Engineering Science ,
Shanghai 201620, P. R. China*

^{b,c}*School of Physics Science and Technology, Xinjiang University,
Urumqi 830046, P. R. China*

Abstract

The relic abundance of asymmetric Dark Matter particles in the scalar–tensor model is analyzed in this article. We extend the numeric and analytic calculation of the relic density of the asymmetric Dark Matter in the standard cosmological scenario to the non-standard cosmological scenario. We focus on the scalar–tensor model. Hubble expansion rate is changed in the nonstandard cosmological scenario. This leaves its imprint on the relic density of Dark Matter particles. In this article we investigate to what extent the asymmetric Dark Matter particle’s relic density is changed in the scalar–tensor model. We use the observed present day Dark Matter abundance to find the constraints on the parameter space in this model.

*wsz08@pku.edu.cn

†Corresponding author, wrns@xju.edu.cn

‡mmtrxt@xju.edu.cn

1 Introduction

The fact that the Universe contains a large amount of non-baryonic Dark Matter is well established by astronomical observations[1, 2, 3]. The Dark Matter has some extraordinary properties, *e.g.*, non-luminous and non-absorbing. Among the various Dark Matter candidate particles, “Weakly Interacting Massive Particles (WIMPs)” are considered to be best motivated candidates since the present Dark Matter relic density can be explained in this scenario naturally [4]. WIMPs are expected to interact among themselves and with the ordinary matter only through the gravity and weak interactions, with masses between 10 GeV to a few TeV. It is assumed that when the universe is radiation dominated, WIMPs are in thermal and chemical equilibrium with the rest of the particles. As the Universe expands and the temperature of the universe drops, the Dark Matter particles decouple from the equilibrium and resulted in essentially constant co-moving density (“freeze-out”). If the entropy of the radiation and matter is conserved during the radiation-dominated era in which the Dark matter particle is produced, the relic abundance of Dark Matter particles can be calculated by solving Boltzmann equation in the standard method. It is shown that for appropriate WIMP annihilation cross section, the resulting relic abundance of Dark Matter is of the same order of magnitude as the observed value.

Most of the WIMPs under consideration are symmetric Dark Matter particles whose particle and anti-particle are the same. The well known example is Neutralino which is Majorana particle appeared in supersymmetric model with conserved R -parity [5]. However, the status of experiment detection of Dark Matter urges people to broaden the search scope. In fact, the idea of asymmetric Dark Matter has been proposed as early as 1980’s[6, 7]. In asymmetric Dark Matter scenario, Dark Matter particles and antiparticles are not identical and have an asymmetry similar to the baryonic asymmetry. Furthermore, it is expected that both asymmetries may have the common origin appeared in the early Universe.

The Dark Matter relic density depends on the characteristics of the Universe, especially the expansion rate of the Universe before Big Bang Nucleosynthesis [8]. The expansion rate may be changed through additional contributions to the total energy density[9], anisotropic expansion [10] and a modification of general relativity [10, 11]. The relic abundances of asymmetric Dark Matter particles in the standard cosmological scenario are investigated in papers [12, 13]. The asymmetric Dark Matter relic density in some nonstandard cosmological scenarios has been discussed [14, 15]. In scalar-tensor model, it is shown that the relic density of Dark Matter is increased with the changing expansion rate of the Universe[16]. Obviously, more detailed investigation is needed for the relic density of asymmetric Dark Matter in the nonstandard cosmological scenarios to find the effects of the modification of the Hubble rate on asymmetric

Dark Matter.

In this paper, the discussion about the relic density of asymmetric WIMP Dark Matter in the standard cosmological scenario is extended to scalar–tensor model. We are not concerned about the mechanism for the asymmetry and assume that there are more particles than the anti–particles in the beginning. We find that the enhanced Hubble rate in scalar-tensor model changes the relic density of both particles and anti–particles. When the cross section is not large, the deviation of the relic density of particle and anti–particle in scalar–tensor model is not large. They are almost in the same amount at the final temperature for smaller cross section in this model. For large cross section, the relic density of anti–particle is depressed and there are only particles left at the final temperature. In the end, the observed present day Dark Matter abundance is applied to constrain the parameter space in the scalar–tensor model.

This paper is arranged as follows. In section 2, the relic density of asymmetric Dark Matter in scalar–tensor model is discussed. In section 3, we constrained the expansion rate in scalar–tensor model using the observed Dark Matter abundance. The conclusions and discussions are given in section 4.

2 Relic Abundance of Asymmetric Dark Matter in the Scalar–Tensor Model

Nonstandard cosmological scenarios are based on the alternative theories of gravity rather than the General Relativity. The scalar–tensor theories are the well studied alternative theories of gravity. In scalar–tensor model, the gravity sector is extended to contain an extra scalar field ϕ which couples to the matter fields through the metric tensor. It is shown that in such models with a single matter sector there is an enhancement of H before BBN [16, 17]. Typically the expansion rate H in these models is given by [16]:

$$H = f_\phi(T)H_{\text{std}}, \quad (1)$$

where $f_\phi(T) \simeq 2.19 \times 10^{14} (T_0/T)^{0.82}$ is an enhancement factor and T_0 is the present temperature of the Universe. In terms of new variable $x = m_\chi/T$ where m_χ is the mass of the Dark Matter particles χ and $\bar{\chi}$, this factor is expressed as $f_\phi(x) \simeq 9.65 \times 10^3 (\text{GeV}/m_\chi)^{0.82} x^{0.82}$. Here $H_{\text{std}} = \sqrt{8\pi^3 g_*/90} T^2/M_{\text{P}} \equiv H(m_\chi)/x^2$ with $H(m_\chi) = \sqrt{8\pi^3 g_*/90} m_\chi^2/M_{\text{P}}$, g_* is the effective number of the relativistic degrees of freedom. At the low temperature T_{tr} , the factor $f_\phi(T)$ must tend to 1 so that the standard cosmology resumes [16]. T_{tr} is called the transition temperature at which point the Hubble expansion rate is returned to the standard Hubble rate.

The abundances of asymmetric Dark Matter χ and $\bar{\chi}$ are characterized by the number densities n_χ , $n_{\bar{\chi}}$, respectively, here $\bar{\chi} \neq \chi$. The relic densities of χ and $\bar{\chi}$ are obtained by solving their Boltzmann equations respectively. The Boltzmann equations describe the time evolution of the number densities n_χ , $n_{\bar{\chi}}$ in the expanding universe. Based on our assumption that only $\chi\bar{\chi}$ pairs can annihilate into Standard Model (SM) particles, while $\chi\chi$ and $\bar{\chi}\bar{\chi}$ pairs can not, the Boltzmann equations are:

$$\begin{aligned}\frac{dn_\chi}{dt} + 3Hn_\chi &= -\langle\sigma v\rangle(n_\chi n_{\bar{\chi}} - n_{\chi,\text{eq}}n_{\bar{\chi},\text{eq}}); \\ \frac{dn_{\bar{\chi}}}{dt} + 3Hn_{\bar{\chi}} &= -\langle\sigma v\rangle(n_\chi n_{\bar{\chi}} - n_{\chi,\text{eq}}n_{\bar{\chi},\text{eq}}),\end{aligned}\quad (2)$$

where $\langle\sigma v\rangle$ is the thermally averaged annihilation cross section times relative velocity of the annihilating particles. $n_{\chi,\text{eq}} = g_\chi (m_\chi T/2\pi)^{3/2} e^{-(m_\chi + \mu_\chi)/T}$ and $n_{\bar{\chi},\text{eq}} = g_{\bar{\chi}} (m_\chi T/2\pi)^{3/2} e^{-(m_\chi - \mu_\chi)/T}$ are the equilibrium number density for particle and anti-particle, where g_χ is the number of the internal degrees of freedom of χ and $\bar{\chi}$ particles. In equilibrium state, the chemical potential of the particles and anti-particles are assumed to be $\mu_{\bar{\chi}} = -\mu_\chi$.

Usually it is assumed that at high temperature, χ and $\bar{\chi}$ particles are in thermal equilibrium in the early universe. Following the expansion of the universe, the temperature drops down. The number densities $n_{\chi,\text{eq}}$ and $n_{\bar{\chi},\text{eq}}$ decrease exponentially for $m_\chi > |\mu_\chi|$ when $T < m_\chi$. When the interaction rates $\Gamma = n_\chi \langle\sigma v\rangle$ for particle and $\bar{\Gamma} = n_{\bar{\chi}} \langle\sigma v\rangle$ for anti-particle drop below the Hubble expansion rate H , χ and $\bar{\chi}$ particles decouple from chemical equilibrium and their co-moving number densities are fixed. The temperature at this decoupling point is called the ‘‘freeze-out’’ temperature.

Next we reformulate the Boltzmann equations (2) in terms of the dimensionless quantities $Y_\chi = n_\chi/s$, $Y_{\bar{\chi}} = n_{\bar{\chi}}/s$ for convenience. The entropy density s is given by $s = (2\pi^2/45)g_*T^3$. If we furthermore assume $dg_*/dx \simeq 0$ during the radiation-dominated period, the Boltzmann equations (2) become

$$\frac{dY_\chi}{dx} = -\frac{\lambda\langle\sigma v\rangle}{x^2 f_\phi(x)} (Y_\chi Y_{\bar{\chi}} - Y_{\chi,\text{eq}} Y_{\bar{\chi},\text{eq}}); \quad (3)$$

$$\frac{dY_{\bar{\chi}}}{dx} = -\frac{\lambda\langle\sigma v\rangle}{x^2 f_\phi(x)} (Y_\chi Y_{\bar{\chi}} - Y_{\chi,\text{eq}} Y_{\bar{\chi},\text{eq}}), \quad (4)$$

where we have introduced the constant

$$\lambda = \frac{x^3 s}{H(m_\chi)} = \sqrt{\frac{\pi}{45}} g_* m_\chi M_{\text{P}}. \quad (5)$$

From Eqs.(3), (4) we obtain

$$Y_\chi - Y_{\bar{\chi}} = C, \quad (6)$$

where C is a constant. This means that the difference of the co-moving densities of the particles and anti-particles is conserved. Considering the relation (6), the Boltzmann equations (3) and

(4) become

$$\frac{dY_\chi}{dx} = -\frac{\lambda\langle\sigma v\rangle}{x^2 f_\phi(x)} (Y_\chi^2 - CY_\chi - P); \quad (7)$$

$$\frac{dY_{\bar{\chi}}}{dx} = -\frac{\lambda\langle\sigma v\rangle}{x^2 f_\phi(x)} (Y_{\bar{\chi}}^2 + CY_{\bar{\chi}} - P), \quad (8)$$

where $P = Y_{\chi,\text{eq}}Y_{\bar{\chi},\text{eq}} = (0.145g_\chi/g_*)^2 x^3 e^{-2x}$

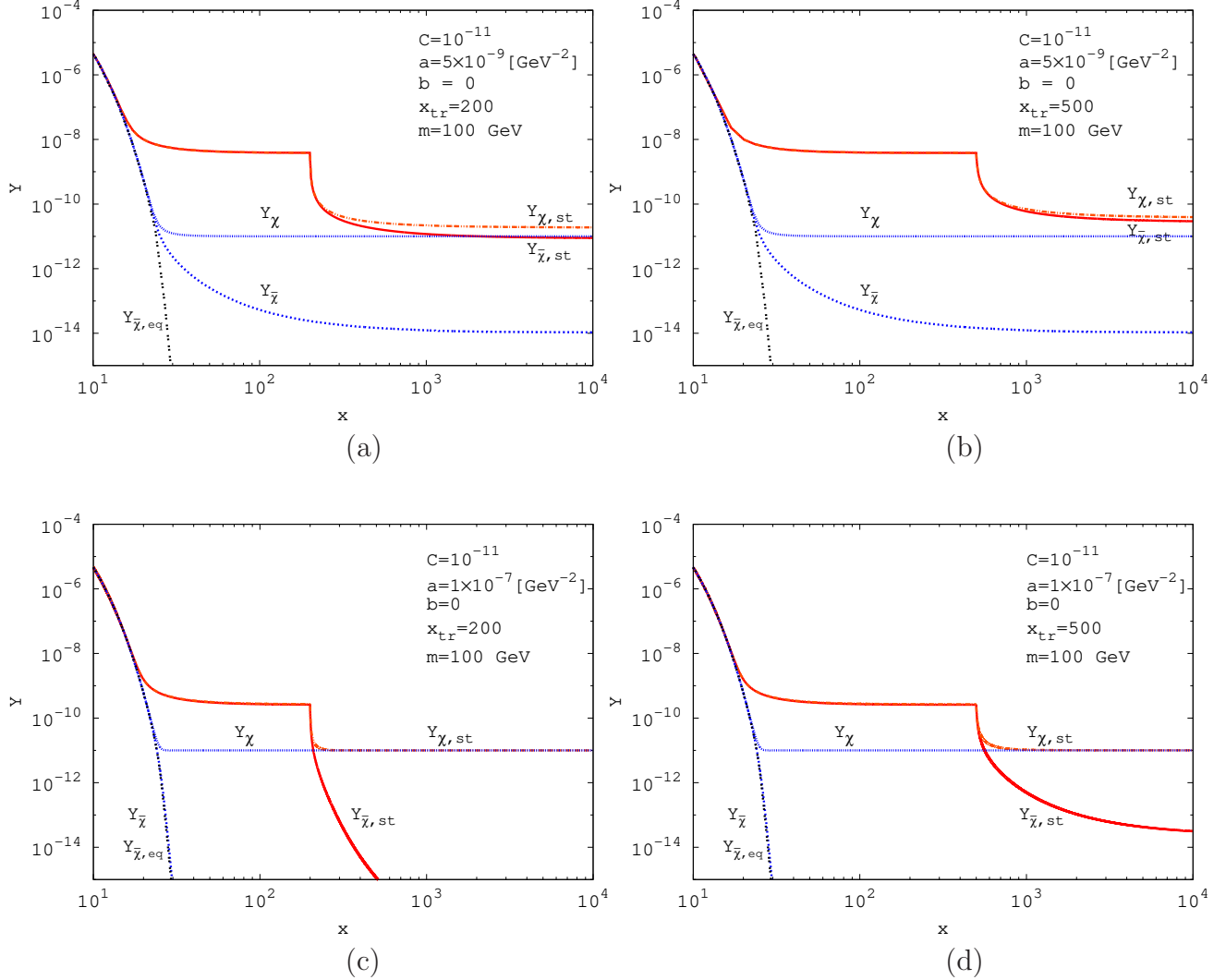


Figure 1: The relic abundance Y as a function of the inverse-scaled temperature $x = m_\chi/T$ for s -wave annihilation ($b=0$). Here $Y_{\chi,\text{st}}$ and $Y_{\bar{\chi},\text{st}}$ are the abundance for particle χ and anti-particle $\bar{\chi}$ in the scalar-tensor model, while Y_χ and $Y_{\bar{\chi}}$ are for the standard cosmological scenario. Panel (a), (c) are for $x_{\text{tr}} = 200$ and panel (b), (d) are for $x_{\text{tr}} = 500$.

Eqs.(7), (8) can be solved numerically. The relic abundance for particle and anti-particle Y as a function of the inverse-scaled temperature $x = m_\chi/T$ for s -wave annihilation is given numerically in Fig.1. The double dotted (black) line is the equilibrium value of the anti-particle abundance. The solid (red) line is the relic abundance for anti-particle and dot-dashed (red)

line is that for the particle in the scalar–tensor model. For comparison, we also give the relic abundance of Dark Matter in the standard cosmological scenario where the dotted (blue) line is the relic abundance for the anti–particle while the short dashed (blue) line for particle. The calculations are carried out for different cross sections and different inverse–scaled transition temperatures $x_{\text{tr}} = m_\chi/T_{\text{tr}}$. In the calculations we take the thermally averaged cross section as $\langle\sigma v\rangle \approx a + 6bx^{-1} + \mathcal{O}(x^{-2})$, where a is dominant for s–wave $\chi\bar{\chi}$ annihilation, while b for p–wave annihilation. In Fig.1 we take $a = 5.0 \times 10^{-9} \text{ GeV}^{-2}$, $b = 0$ for panels (a), (b) and $a = 1 \times 10^{-7} \text{ GeV}^{-2}$, $b = 0$ for (c), (d). In panels (a), (c) we consider $x_{\text{tr}} = 200$ and in panels (b), (d) $x_{\text{tr}} = 500$. In all cases, we take $C = 10^{-11}$, $m_\chi = 100 \text{ GeV}$, $g_\chi = 2$ and $g_* = 90$.

Two common features of the relic abundances in scalar-tensor model can be shown in Fig.1. First, when the inverse–scaled temperature is larger than the inverse–scaled transition temperature the particle and anti–particle abundance are kept in the same amount which are larger than the standard scenario. This is because of the enhancement of the expansion rate in scalar-tensor model. Due to this enhancement, the asymmetric Dark Matter particles freeze–out earlier than the standard case, leading to the increases of particle and anti–particle abundances. For example, the particle abundance is increased as large as 9×10^{-9} in (a) of Fig.1. Because $Y_\chi - Y_{\bar{\chi}} = C$, comparing to asymmetry factor $C = 10^{-11}$, this value is so large that the difference between particle and anti–particle abundance can not be manifested in the figure. Thus it seems that the particle and anti–particle are in the same amount before transition temperature. Second, sudden decreases of the relic abundances in scalar-tensor model appear at the transition temperatures x_{tr} in Fig.1. This corresponds to the behavior of the Hubble parameter in the scalar-tensor model around the transition temperatures T_{tr} . For transition temperatures varying from 1 MeV to a few GeV, the Hubble parameter decreases suddenly by a few orders of magnitude at T_{tr} .

Once the temperature drops below the transition temperature, the Hubble expansion rate is resumed to the standard Hubble rate, and the deviation of the abundance for the particle and anti–particle is appeared. The behavior of the relic abundance is influenced by the cross sections. For smaller s–wave annihilation cross section $a = 5 \times 10^{-9} \text{ GeV}^{-2}$, the relic abundances $Y_{\chi,\text{st}}$ and $Y_{\bar{\chi},\text{st}}$ for particle χ and anti–particle $\bar{\chi}$ in scalar–tensor model are greater than that of the standard case in Fig.1 for both panel (a) and panel (b). When the cross section is larger as $a = 1 \times 10^{-7} \text{ GeV}^{-2}$, the final abundance for particle in scalar–tensor model is same with the standard case; while the anti–particle abundance in scalar–tensor model is decreased sharply as the temperature drops for the transition temperature $x_{\text{tr}} = 200$. The decrease is smaller for the transition temperature $x_{\text{tr}} = 500$. Notice that for the cross section $a = 1 \times 10^{-7} \text{ GeV}^{-2}$ the relic abundance of anti–particle in standard cosmology $Y_{\bar{\chi}}$ are also same as the equilibrium value $Y_{\bar{\chi},\text{eq}}$.

In the following, we give the approximate analytic solutions of the relic densities for asymmetric Dark Matter in scalar-tensor model. The procedure is the same as in standard cosmological scenario [12]. For convenience, we introduce the quantity $\Delta_{\bar{\chi}} = Y_{\bar{\chi}} - Y_{\bar{\chi},\text{eq}}$. Using $\Delta_{\bar{\chi}}$, the Boltzmann equation (8) can be rewritten as:

$$\frac{d\Delta_{\bar{\chi}}}{dx} = -\frac{dY_{\bar{\chi},\text{eq}}}{dx} - \frac{\lambda\langle\sigma v\rangle}{x^2 f_\phi(x)} [\Delta_{\bar{\chi}}(\Delta_{\bar{\chi}} + 2Y_{\bar{\chi},\text{eq}}) + C\Delta_{\bar{\chi}}]. \quad (9)$$

At sufficiently high temperature, $Y_{\bar{\chi}}$ tracks its equilibrium value $Y_{\bar{\chi},\text{eq}}$ very closely. In that regime the quantity $\Delta_{\bar{\chi}}$ is small, and $d\Delta_{\bar{\chi}}/dx$ and $\Delta_{\bar{\chi}}^2$ are negligible. The Boltzmann equation (9) then becomes

$$\frac{dY_{\bar{\chi},\text{eq}}}{dx} = -\frac{\lambda\langle\sigma v\rangle}{x^2 f_\phi(x)} (2\Delta_{\bar{\chi}}Y_{\bar{\chi},\text{eq}} + C\Delta_{\bar{\chi}}). \quad (10)$$

Repeating the same method as in [14], we obtain

$$\Delta_{\bar{\chi}} \simeq \frac{2x^2 f_\phi(x) P}{\lambda\langle\sigma v\rangle (C^2 + 4P)}. \quad (11)$$

Where we used $Y_{\bar{\chi},\text{eq}} = -C/2 + \sqrt{C^2/4 + P}$ which is obtained by solving the Boltzmann equation Eq.(8) in equilibrium state. The freeze-out temperature \bar{x}_F for $\bar{\chi}$ is determined by using this solution.

On the other hand, for sufficiently low temperature, i.e. for $x > \bar{x}_F$, we have $\Delta_{\bar{\chi}} \approx Y_{\bar{\chi}} \gg Y_{\bar{\chi},\text{eq}}$. The terms involving $dY_{\bar{\chi},\text{eq}}/dx$ and $Y_{\bar{\chi},\text{eq}}$ in the Boltzmann equation (9) can be ignored, so that

$$\frac{d\Delta_{\bar{\chi}}}{dx} = -\frac{\lambda\langle\sigma v\rangle}{x^2 f_\phi(x)} (\Delta_{\bar{\chi}}^2 + C\Delta_{\bar{\chi}}). \quad (12)$$

We integrate Eq.(12) from \bar{x}_F to x_{tr} where the scalar-tensor theories applied and from x_{tr} to ∞ in which period the standard cosmology is resumed. Again assuming $\Delta_{\bar{\chi}}(\bar{x}_F) \gg \Delta_{\bar{\chi}}(\infty)$, we have

$$Y_{\bar{\chi}}(x \rightarrow \infty) = \frac{C}{\exp\left[\sqrt{\pi/45} C m_\chi M_{\text{P}} I(\bar{x}_F, x_{\text{tr}})\right] - 1}, \quad (13)$$

where

$$I(\bar{x}_F, x_{\text{tr}}) = \int_{\bar{x}_F}^{x_{\text{tr}}} \frac{\sqrt{g_*}\langle\sigma v\rangle}{x^2 f_\phi(x)} dx + \int_{x_{\text{tr}}}^{\infty} \frac{\sqrt{g_*}\langle\sigma v\rangle}{x^2} dx \quad (14)$$

$$= \sqrt{g_*}[A(\bar{x}_F) - A(x_{\text{tr}}) + B(x_{\text{tr}})], \quad (15)$$

with $A(x) = (m_\chi/\text{GeV})^{0.82}(5.6938 \times 10^{-5} a x^{-1.82} + 2.2048 \times 10^{-4} b x^{-2.82})$, $B(x) = ax^{-1} + 3bx^{-2}$. The relic abundance for χ particle is obtained from Eq.(6) as

$$Y_\chi(x \rightarrow \infty) = \frac{C}{-\exp\left[-\sqrt{\pi/45} C m_\chi M_{\text{P}} I(x_F, x_{\text{tr}})\right] + 1}, \quad (16)$$

We note that only if $x_F = \bar{x}_F$, Eqs.(13) and (16) are consistent each other with the constraint (6).

The final Dark Matter abundance can be expressed in a more canonical form as usual:

$$\Omega_\chi h^2 = \frac{m_\chi s_0 Y_\chi(x \rightarrow \infty) h^2}{\rho_{\text{cr}}}, \quad (17)$$

with $s_0 = 2.9 \times 10^3 \text{ cm}^{-3}$ being the present entropy density, and $\rho_{\text{cr}} = 3M_{\text{P}}^2 H_0^2 / (8\pi)$ the present critical density, where H_0 is the Hubble constant. The present relic density for Dark Matter is then predicted as

$$\Omega_{\text{DM}} h^2 = \frac{2.76 \times 10^8 m_\chi C}{\exp \left[\sqrt{\pi/45} C m_\chi M_{\text{P}} I(\bar{x}_F, x_{\text{tr}}) \right] - 1} - \frac{2.76 \times 10^8 m_\chi C}{\exp \left[-\sqrt{\pi/45} C m_\chi M_{\text{P}} I(x_F, x_{\text{tr}}) \right] - 1}. \quad (18)$$

We need to fix the freeze-out temperature in order to calculate the final relic density. When the deviation $\Delta_{\bar{\chi}}$ is of the same order as the equilibrium value of $Y_{\bar{\chi}}$, the freeze-out occurs:

$$\xi Y_{\bar{\chi}, \text{eq}}(\bar{x}_F) = \Delta_{\bar{\chi}}(\bar{x}_F), \quad (19)$$

where \bar{x}_F is the freeze-out temperature which is obtained by solving Eq.(19) and ξ is a numerical constant of order unity, $\xi = \sqrt{2} - 1$ [18]. Using Eq.(11), the freeze-out temperature \bar{x}_F is determined for $\bar{\chi}$ particles.

3 Constraints on Parameter Space

Nine-year Wilkinson Microwave Anisotropy Probe (WMAP) observations give the Dark Matter relic density as [3]

$$\Omega_{\text{DM}} h^2 = 0.1138 \pm 0.0045, \quad (20)$$

where Ω_{DM} is the Dark Matter (DM) density in units of the critical density, and $h = 0.738 \pm 0.024$ is the Hubble constant in units of $100 \text{ km}/(\text{s} \cdot \text{Mpc})$. In this section, we use this result to find the constraints on the parameter space of scalar-tensor model. For asymmetric Dark Matter, the particle χ and anti-particle $\bar{\chi}$ relic density account for total Dark Matter density,

$$\Omega_{\text{DM}} = \Omega_\chi + \Omega_{\bar{\chi}}. \quad (21)$$

According to Eq.(20), we use the following range,

$$0.10 < \Omega_{\text{DM}} h^2 < 0.12. \quad (22)$$

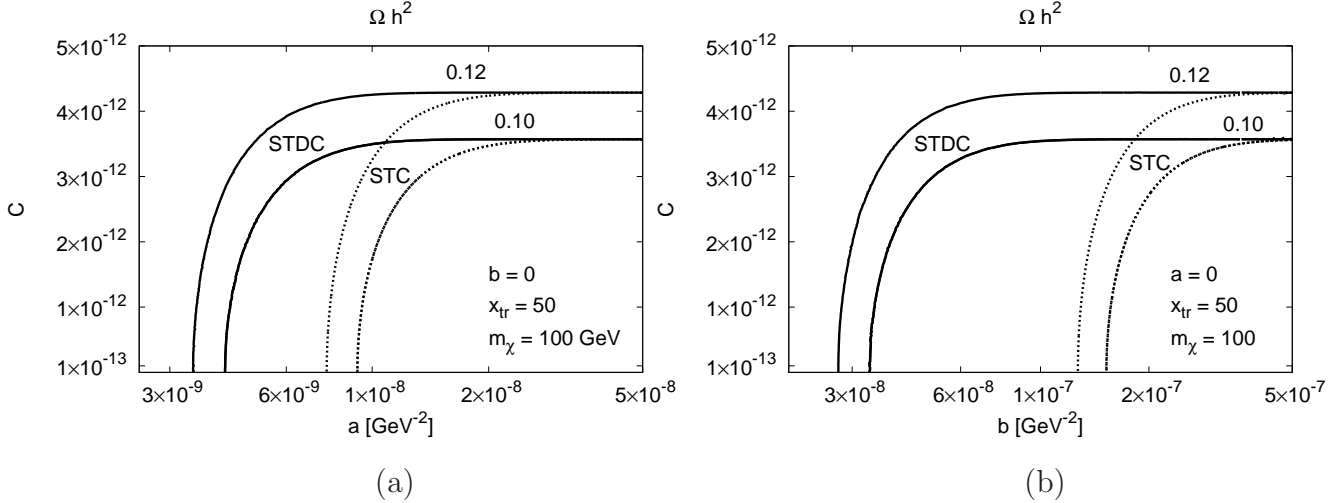


Figure 2: The allowed region in the (a, C) plane for $b = 0$ (left) and in the (b, C) plane for $a = 0$ (right), when the Dark Matter density $\Omega_{\text{DM}}h^2$ lies between 0.10 and 0.12. Here we take $m_\chi = 100$ GeV, $g_\chi = 2$ and $g_* = 90$, $x_{\text{tr}} = 50$. The solid lines are for the standard cosmological scenario (STDC), and the dotted lines are for scalar–tensor cosmology (STC).

Fig.2 shows the relation between the annihilation cross section parameters a, b and the asymmetry factor C when the Dark Matter relic density $\Omega_{\text{DM}}h^2$ lies between 0.10 and 0.12. Here we take $m_\chi = 100$ GeV, $g_\chi = 2$ and $g_* = 90$, $x_{\text{tr}} = 50$. The solid lines are for the standard cosmological scenario (STDC), the dotted lines are for the scalar–tensor cosmology (STC). In the left frame (a) of Fig.2, it is shown that for the values of s–wave annihilation cross sections from $a = 3.5 \times 10^{-9}$ GeV $^{-2}$ to $a = 5.0 \times 10^{-8}$ GeV $^{-2}$, the observed Dark Matter abundance is obtained for the range of C from 0 to 4.3×10^{-12} for the standard cosmology. The initial cross–section is increased to $a = 7.7 \times 10^{-9}$ GeV $^{-2}$ for the scalar–tensor cosmology to obtain the observed Dark Matter abundance. In the right frame (b) of Fig.2, for the asymmetry factor C from 0 to 4.4×10^{-12} , one needs the p–wave annihilation cross sections from $b = 2.7 \times 10^{-8}$ GeV $^{-2}$ to $b = 5.0 \times 10^{-7}$ GeV $^{-2}$ to obtain the observed Dark Matter abundance for standard cosmology. For the scalar–tensor model, the corresponding p–wave cross section ranges from $b = 1.3 \times 10^{-7}$ GeV $^{-2}$ to $b = 5.0 \times 10^{-7}$ GeV $^{-2}$. The cross section is increased evidently for the scalar–tensor cosmology for both s–wave annihilation and p–wave annihilation cross sections to obtain the observed Dark Matter abundance. This is because in scalar–tensor model the interaction rate is larger than the standard scenario. Asymmetric Dark Matter particles need larger annihilation cross sections in order to fall in the observation range.

Fig.3 shows the allowed region in the (m_χ, C) plane when the Dark Matter density $\Omega_{\text{DM}}h^2$ lies between 0.10 and 0.12. Here $a = 5 \times 10^{-8}$ GeV $^{-2}$, $b = 0$, $x_{\text{tr}} = 50$. When the mass of the Dark Matter increases from 50 to 450 GeV, the asymmetry factor C decreases from

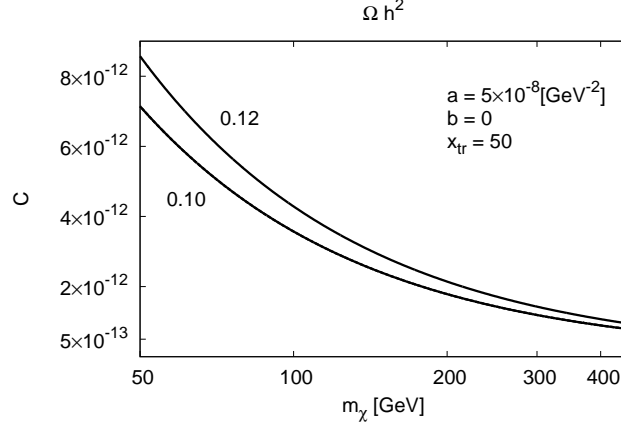


Figure 3: The allowed region in the (m_χ, C) plane when the Dark Matter density Ωh^2 lies between 0.10 and 0.12. Here we take $a = 5 \times 10^{-8} \text{ GeV}^{-2}$, $b = 0$, $x_{\text{tr}} = 50$.

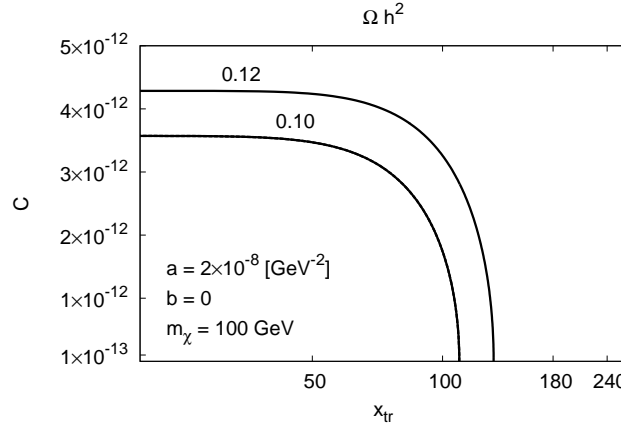


Figure 4: The allowed region in the (x_{tr}, C) plane for $a = 2 \times 10^{-8} \text{ GeV}^{-2}$, $b = 0$, $m_\chi = 100 \text{ GeV}$ when the Dark Matter density Ωh^2 lies between 0.10 and 0.12.

$C = 8.5 \times 10^{-12}$ to $C = 8.0 \times 10^{-13}$ to obtain the observed Dark Matter relic density. This can be understood from Eq.(18). When m_χ increases, C is decreased in order to keep the observed Dark Matter abundance.

The constraint of observed Dark Matter relic density on the transition temperature in the scalar-tensor model is plotted in Fig.4. The allowed region in the (x_{tr}, C) plane for $a = 2 \times 10^{-8} \text{ GeV}^{-2}$, $b = 0$, $m_\chi = 100 \text{ GeV}$ is shown when the Dark Matter relic density $\Omega_{\text{DM}} h^2$ lies between 0.10 and 0.12. When the inverse-scaled transition temperature x_{tr} of the asymmetric Dark Matter in the scalar-tensor model increases from 20 to 130, the asymmetry factor C decreases from $C = 4.3 \times 10^{-12}$ to 0 to obtain the observed Dark Matter relic density. This means that when the inverse-scaled transition temperature increases the observed Dark Matter relic

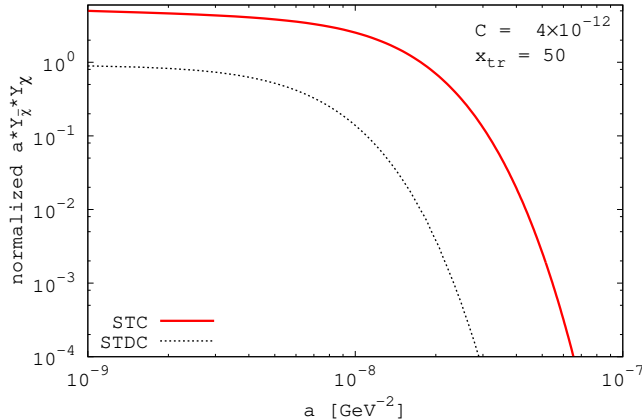


Figure 5: Annihilation rate for asymmetric Dark Matter in scalar–tensor cosmology and standard cosmology divided by the same quantity for symmetric Dark Matter ($C = 0$), as a function of a . The solid (red) line is for the scalar–tensor cosmology and the dotted (black) line for the standard cosmology. Here $b = 0$, $m_\chi = 100$ GeV and $C = 4 \times 10^{-12}$, $x_{\text{tr}} = 50$, $g_\chi = 2$, $g_* = 90$.

density can be compensated by taking smaller asymmetry factor C .

The asymmetric Dark Matter can be detected by the direct detection. Indirect detection for asymmetric Dark Matter in the standard cosmological scenario, however, can not be used. This is because in the standard scenario the symmetric part of the asymmetric Dark Matter annihilated away with its anti–particles in the early universe and only particles left in the present universe. For the non–standard cosmological scenario like scalar–tensor cosmology, there are still quite sizable amount of anti–particles left. Of course the left amount of anti–particles mostly depends on the size of annihilation cross section. Annihilation rate for asymmetric Dark Matter is $\Gamma \propto \langle \sigma v \rangle Y_{\bar{\chi}} Y_\chi$. Fig.5 shows the annihilation rate for asymmetric Dark Matter in scalar–tensor cosmology and standard cosmology which is divided by the same quantity for the symmetric Dark Matter $C = 0$. The solid (red) line is for scalar–tensor cosmology and the dotted (black) line is for standard cosmology. We found the normalized annihilation rate is increased for scalar–tensor cosmology comparing to the standard one. We take an example, for $a = 10^{-8}$ GeV, the corresponding normalized annihilation rate is 0.14 for standard cosmology and 2.52 for scalar–tensor cosmology. This behavior makes the indirect detection possible for scalar–tensor cosmology. For the larger cross section as $a \sim 1 \times 10^{-7}$ GeV $^{-2}$, the relic density of anti–particles at the present day are almost depressed for scalar–tensor cosmology too. This is indeed demonstrated in Fig.1 (c), (d). Therefore we emphasize that the indirect detection signal constraints like Fermi–LAT [19] can be used to nonstandard cosmological scenarios like scalar–tensor model in conditionally.

4 Summary and Conclusions

In this paper we investigate the relic abundance of asymmetric WIMP Dark Matter in scalar-tensor model. For asymmetric Dark Matter, the Dark Matter particles and anti-particles are distinct. In the standard cosmological scenario, it is assumed that the particles were in thermal equilibrium in the early universe and decoupled when they were non-relativistic. The discussion of the relic density of asymmetric Dark Matter in the standard cosmological scenario is extended to nonstandard cosmological scenario. Specifically we discuss the scalar-tensor model. The expansion rate is enhanced in scalar-tensor model and it leaves its imprint on the relic density of asymmetric Dark Matter.

In this work, we give the exact numerical solutions and approximate analytical solutions of the relic abundances for asymmetric Dark Matter in scalar-tensor model. It is shown that the relic abundances for particles and anti-particles in scalar-tensor model are both greater than that of the standard cosmology. This is because the expansion rate is enhanced in scalar-tensor model. The particles and anti-particles freeze-out earlier than the standard case, leading to the increases of particle and anti-particle abundances. A significant feature of the relic abundances in scalar-tensor model is the sudden decrease at the transition temperatures x_{tr} in which the Hubble parameter returns to the standard cosmology.

We furthermore investigate the constraints on the transition temperature and the asymmetry factor in the scalar-tensor model using the observed Dark Matter abundance. The cross section is increased approximately one order in scalar-tensor model in order to obtain the observed Dark Matter abundance comparing to the standard cosmological scenario for asymmetric Dark Matter. When the mass of the asymmetric Dark Matter particles increases the asymmetry factor C is decreased to compensate the observed Dark Matter abundance. If we take $a = 2 \times 10^{-8} \text{ GeV}^{-2}$, $b = 0$, $m_\chi = 100 \text{ GeV}$, the inverse-scale transition temperature x_{tr} of the asymmetric Dark Matter in the scalar-tensor model increases from 20 to 130 as the asymmetry factor C decreases from $C = 4.3 \times 10^{-12}$ to 0 to obtain the observed Dark Matter relic density.

It is important to understand the relic abundance of asymmetric Dark Matter in the early universe in nonstandard cosmological models. Our work gives the constraints on the parameter space for the scalar-tensor model in asymmetric Dark Matter case. Indirect detection signal is possible for the nonstandard cosmological scenarios due to the enhanced annihilation rate..

Acknowledgments

The work of Shun-Zhi Wang is supported by Shanghai University of Engineering Science under grant No.11XK11 and No.2011XZ10. The work of H. Iminniyaz is supported by the National Natural Science Foundation of China (11365022, 11047009). Mamatrishat Mamat is supported by National Natural Science Foundation of China (61366001).

References

- [1] F. Zwicky, *Astrophys. J.* **86**, 217(1937).
- [2] G. Bertone, D. Hooper, and J. Silk, *Phys. Rept.* **405**,279 (2005).
- [3] G. Hinshaw *et al.* [WMAP Collaboration], *Astrophys. J. Suppl.* **208**, 19 (2013); C. L. Bennett *et al.* [WMAP Collaboration], *Astrophys. J. Suppl.* **208**, 20 (2013).
- [4] For a review, see K. A. Olive *et al.* (PDG), *Chin. Phys.* **C38**, 090001 (2014)
- [5] For a review, see G. Jungman, M. Kamionkowski, and K. Griest, *Phys. Rep.* **267**, 195 (1996)
- [6] S. Nussinov, *Phys. Lett. B* **165**, 55 (1985); K. Griest and D. Seckel. *Nucl. Phys. B* **283**, 681 (1987); S. M. Barr, R. S. Chivukula and E. Farhi, *Phys. Lett. B* **241**, 387 (1990); R. S. Chivukula and T. P. Walker, *Nucl. Phys. B* **329**, 445 (1990); D. B. Kaplan, *Phys. Rev. Lett.* **68**, 742 (1992); D. Hooper, J. March-Russell and S. M. West, *Phys. Lett. B* **605**, 228 (2005) [arXiv:hep-ph/0410114]; *JCAP* **0901** (2009) 043 [arXiv:0811.4153v1 [hep-ph]]; H. An, S. L. Chen, R. N. Mohapatra and Y. Zhang, *JHEP* **1003**, 124 (2010) [arXiv:0911.4463 [hep-ph]]; T. Cohen and K. M. Zurek, *Phys. Rev. Lett.* **104**, 101301 (2010) [arXiv:0909.2035 [hep-ph]]. D. E. Kaplan, M. A. Luty and K. M. Zurek, *Phys. Rev. D* **79**, 115016 (2009) [arXiv:0901.4117 [hep-ph]]; T. Cohen, D. J. Phalen, A. Pierce and K. M. Zurek, *Phys. Rev. D* **82**, 056001 (2010) [arXiv:1005.1655 [hep-ph]]; J. Shelton and K. M. Zurek, *Phys. Rev. D* **82**, 123512 (2010) [arXiv:1008.1997 [hep-ph]];
- [7] A. Belyaev, M. T. Frandsen, F. Sannino and S. Sarkar, *Phys. Rev. D* **83**, 015007 (2011) [arXiv:1007.4839].
- [8] G. Giudice, E. Kolb, and A. Riotto *Phys. Rev. D* **64** (2001) 023508 [arXiv:hep-ph/0005123]; N. Fornengo, A. Riotto, and S. Scopel *Phys. Rev. D* **67** (2003) 023514 [arXiv:hep-ph/0208072]; C. Pallis *Astropart. Phys.* **21** (2004) 689 [arXiv:hep-ph/0402033]; G. Gelmini and P. Gondolo, *Phys. Rev. D* **74** (2006) 023510 [arXiv:hep-ph/0602230]; M. Drees, H. Iminniyaz and M. Kakizaki, *Phys. Rev. D* **73**

- (2006) 123502 [arXiv:hep-ph/0603165]; G. Gelmini *et al* Phys. Rev. D **74** (2006)083514 [hep-ph/0605016].
- [9] P. Salati, Phys. Lett. B **571**, 121 (2003) [astro-ph/0207396].
- [10] M. Kamionkowski and M. S. Turner, Phys. Rev. D **42**, 3310 (1990).
- [11] R. Catena, N. Fornengo, A. Masiero, M. Pietroni and F. Rosati, Phys. Rev. D **70**, 063519 (2004) [arXiv:astro-ph/0403614].
- [12] H. Iminiyaz, M. Drees and X. Chen, JCAP **1107**, 003 (2011) [arXiv:1104.5548 [hep-ph]].
- [13] M. L. Graesser, I. M. Shoemaker and L. Vecchi, JHEP **1110**, 110 (2011) [arXiv:1103.2771 [hep-ph]].
- [14] H. Iminiyaz and X. Chen, Astropart. Phys. **54**, 125 (2014) [arXiv:1308.0353 [hep-ph]].
- [15] G. B. Gelmini, J. H. Huh and T. Rehagen, arXiv:1304.3679 [hep-ph].
- [16] R. Catena *et al.* N. Fornengo, A. Masiero, M. Pietroni and F. Rosati, Phys. Rev. D **70** (2004) 063519 [arXiv:astro-ph/0403614].
- [17] D. Santiago, D. Kalligas and R. Wagoner, Phys. Rev. D **58** (1998) 124005.
- [18] R. J. Scherrer and M. S. Turner, Phys. Rev. D **33**, 1585 (1986), Erratum-ibid. D **34**, 3263 (1986).
- [19] M. Ackermann *et al.* [Fermi-LAT Collaboration], Phys. Rev. Lett. **107**, 241302 (2011) [arXiv:1108.3546 [astro-ph.HE]].